Nano Energy 60 (2019) 449–456

Contents lists available at ScienceDirect

Nano Energy

journal homepage: www.elsevier.com/locate/nanoen

Full paper

Mechano-neuromodulation of autonomic pelvic nerve for underactive bladder: A triboelectric neurostimulator integrated with flexible neural clip interface

Sanghoon Lee[a,b,c,d,1], Hao Wang[b,d,e,1], Wendy Yen Xian Peh[c], Tianyiyi He[b,d,e], Shih-Cheng Yen[b,c], Nitish V. Thakor[b,c,f,g], Chengkuo Lee[b,c,d,e,f,*]

[a] Department of Robotics Engineering, Daegu Geongbuk Institute of Science and Technology (DGIST), Daegu, 42988, Republic of Korea
[b] Department of Electrical and Computer Engineering, National University of Singapore (NUS), 117583, Singapore
[c] Singapore Institute for Neurotechnology (SINAPSE), National University of Singapore, 117456, Singapore
[d] Center for Intelligent Sensors and MEMS, National University of Singapore (NUS), Singapore, 117576
[e] NUS Suzhou Research Institute (NUSRI), Suzhou, Industrial Park, Suzhou, 215123, PR China
[f] Graduate School for Integrative Science and Engineering, National University of Singapore (NUS), 117456, Singapore
[g] Johns Hopkins University, Biomedical Engineering, Baltimore, MD, 21205, USA

ARTICLE INFO

Keywords:
Triboelectric nanogenerator
Neural clip interface
Pelvic nerve
Underactive bladder
Mechano-neuromodulation

ABSTRACT

Mechano-neuromodulation of autonomic pelvic nerves was demonstrated for the first time using a triboelectric neurostimulator integrated with flexible neural clip interface. The detailed stimulation parameters such as current, pulse width, and charges generated by the proposed TENG were investigated for the stimulation of autonomic pelvic nerve. In *in vivo* experiments, different beats per minute (BPM) were delivered to the nerves to investigate the effect of stimulation frequency on mechano-neurostimulation while monitoring changes in bladder pressure and the occurrence of micturition. Furthermore, different numbers of pulses were applied to stimulate the pelvic nerve. The bladder contractions with micturition were observed when applying more than 50 BPM as well as one pulse. Comparison of stimulation was performed using a commercial stimulator with the similar long-pulse widths as generated by TENGs. In addition, chronic implantation of flexible clip interface was demonstrated with functionality test of the interface. The results demonstrate that this technology may potentially be used for self-powered mechano-neuromodulation for bladder function in the future.

1. Introduction

Technology advances in flexible materials and cutting-edge electronics have greatly promoted the development of diversified flexible electronics for the collection of biological information of human. Due to the superior advantages over its rigid counterparts, flexible electronics can be comfortably stuck on the surface of human skin and/or even implanted inside human body with biocompatible encapsulation, i.e., wearable electronics and implantable electronics [1–5]. Along the past few years, various flexible wearable electronics have been developed with a broad range of functionalities, e.g., information sensing of pressure, strain, temperature, pulse/heart rate and sweat [6–9], drug delivery [10,11], ECG/EMG recording [12], and wearable energy harvesting [13–15]. Meanwhile, flexible implantable electronics also receive grand research effort to achieve the functionalities in a more direct and efficient manner for clinical applications, for example, physiological signal recording by implanted electrodes and sensors [16–20], cellular/neural/muscle stimulation [21–29], organ actuation [30], and implantable energy harvesting [31–36]. Flexible wearable and implantable electronics provide a more comfortable way of interaction between human body and devices in terms of recording and treatment of physiological conditions, improving the life quality of millions of people.

Implantable electronics can potentially treat the underactive bladder (UAB) syndrome, which is caused by a few risk factors such as aging, neurologic diseases, and diabetes. UAB defines a group of symptoms including prolonged/failed bladder emptying within a normal time span [37]. Despite all of the serious consequences of UAB, current solutions, the most common being ureteric catheterization, are all accompanied by serious shortcomings [38,39]. With *in vivo*

* Corresponding author. Department of Electrical and Computer Engineering, National University of Singapore (NUS), 117583, Singapore.
E-mail address: elelc@nus.edu.sg (C. Lee).
[1] Both authors contributed equally.

https://doi.org/10.1016/j.nanoen.2019.03.082
Received 24 February 2019; Received in revised form 22 March 2019; Accepted 25 March 2019
Available online 27 March 2019
2211-2855/

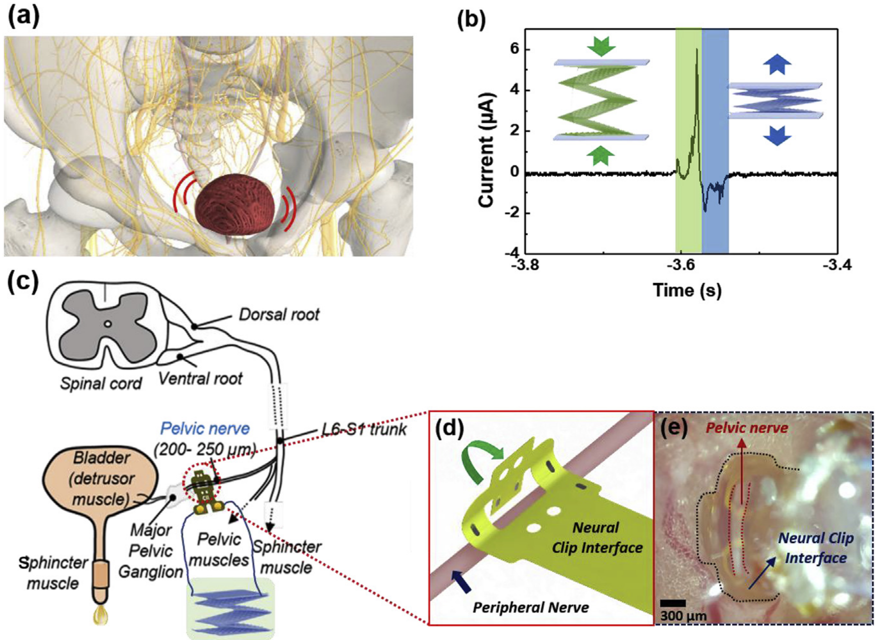

Fig. 1. Conceptual illustration of mechano-neuromodulation. (a) Schematic diagram of bladder in human body. (b) Schematic diagram of operating triboelectric nanogenerator (TENG) and output signals generated by TENG. (c) Schematic diagram of spinal cord, bladder, and bladder nerves and the implantation of triboelectric neuromodulation integrated with flexible neural clip (FNC). (d) Schematic diagram of implanting FNC on a nerve. (e) A microscope image of the implanted FNC on a pelvic nerve in a rat.

experiments, our team has successfully demonstrated a few versions of shape-memory-alloy (SMA) based 3D printed actuators to void bladder with sustainable high efficiency. We also provide proof-of-concept self-control system by having triboelectric nanogenerator (TENG) sensor for indirectly detecting the fullness of bladder for neurogenic UAB patients with degraded nerve function [30,40].

Furthermore, recent interest in neuromodulation using neural interfaces and bioelectronics has focused on autonomic nerves that enable therapeutic effects by regulating extensive functions implicated in organ physiology and chronic disease states [19,41,42]. Specifically, neural signals passing through nerve fibers can be tuned for therapeutic intervention on the human bodily function or chronic disease by reading neural information and stimulating targeted fibers for desired neural signals, or inhibiting unwanted neural signals. One of interests in this field is to modulate and treat bladder dysfunction which is an emerging issue as a major health care problem in aging society [43]. The function of the urinary bladder is to store and expel urine, which is complicatedly controlled by the central, peripheral, and autonomic nervous system [10]. Regarding the UAB patients, again, the damage of these nerves caused by diabetes, infections, or injury of brain/spinal cord results in neurogenic bladder dysfunction [40]. Although several treatments methods have been used in UAB, including behavioral modification, pharmacological treatment, and surgical interventions, neurostimulation methods has emerged as one of the promising technology that regulate bladder function [11]. Electrical stimulation of the autonomic pelvic nerve, which provides a more direct and specific control of bladder contraction than central nerve targets or afferent fibers, shows more effective bladder emptying [12]. This approach is a promising solution for UAB syndrome prolonging or failing bladder voiding.

Implantable stimulators such as pacemaker, cochlear implants, and sacral neuromodulation system (SNS) have been used to stimulate organs or nerves to support or control the bodily functions. It consists of a stimulator, leads (electrodes), and programs to adjust stimulation parameters. The stimulator includes electronic circuits that generate proper stimulation pulses (typically square pulses). This consumes power and requires batteries, making long-term use of implantable stimulators difficult. The battery should generally be replaced after 3–5 years. For instance, an interstim system (InterStim™) for sacral nerve stimulation has the battery lasting for 5 years, so that the battery will need to be replaced [44]. For sustainable and long-tern use of such devices, triboelectric nanogenerators (TENGs) have been demonstrated to scavenge the movements of internal organs, e.g. heart, lung, and diaphragm [13–16]. As a power source for neurostimulation, a piezoelectric energy harvester was applied for deep brain stimulation [17,18], and TENGs that generates exponential wave stimulated peripheral motor nerves [19,20]. However, there is the lack of research associated with stimulation parameters generated by TENGs such as pulse width, current, and frequency that are important factors especially for autonomic nerve stimulation.

In this paper, mechano-neuromodulation of bladder using a stacked TENG combined with a flexible neural clip (FNC) interface is investigated. We characterize detailed stimulation parameters generated by the TENG in terms of current, pulse width, and charge. In *in vivo* experiments, different beats per minute (BPM) of stimulation signals as well as different number of pulses are delivered to the pelvic nerve through the FNC while monitoring bladder pressure changes and the occurrence of micturition. Furthermore, comparison of bladder stimulation by commercial stimulator is demonstrated. Finally, we demonstrate chronic implantation of FNC with histological test, then stimulate bladder.

2. System and device configuration, and *in vivo* demonstration

A human creates various mechanical movements inside or outside the body. The concept of mechano-neuromodulation is that this kind of mechanical movements could be used as an energy source for neuromodulation. Intentional movement generates an output signal by the proposed stimulator, which is transmitted to the target nerves via neural interfaces for electrical stimulation of the nerves, resulting in muscle activations. This evoked mechanical movement probably could be used as an another energy source for possibly continuing other neuromodulation (Fig. 1a). Here, we propose the prototype of a mechano-neuromodulator combined a stacked TENG and FNC interface for bladder modulation. The handheld sizes of TENGs are prepared for easy use in multiple experiments. It can easily grasp with one hand, and it generates electrical signals by pressing and releasing by fingers (Fig. 1b). We demonstrate the modulation of bladder function with the proposed triboelectric neuromodulator by implanting FNC interface in a pelvic nerve of a rat (Fig. 1c). The FNC provides reliable interface on very small pelvic nerve by quickly clipping on it (Fig. 1d). In addition, after the implantation, the FNS provides a stable stimulation interface by adapting to the movement of bladder during micturition (Fig. 1e) [45].

For the TENG, a PET sheet was used as the body of the device with a zigzag shaped structure. This structure provided mechanical support to maintain the shape for multiple experiments. Polytetrafluoroethylene (PTFE) was used as a negative triboelectric material as well as aluminum (Al) foil was used as positive triboelectric material to achieve the maximum output. Total 4-layer TENGs were prepared, which considers the length of the released device compatible to one-hand operation. To generate different electrical energies, different sizes of contact areas (1 cm^2, 4 cm^2, and 16 cm^2) were prepared (Suppl. Fig. 1). The detailed configuration and characterization are described in supplementary. The detailed operation mechanism was described in previous work [20].

Flexible neural clip interfaces were fabricated by conventional microfabrication technology. It consisted of a polyimide-Au-polyimide sandwiched structure (Suppl. Fig. 2a). This unique design of the device enabled them to be easily and reliably implanted on small pelvic nerves (diameter: ~250 μm) in rats (Fig. 1e). Two gold electrodes of the device were opened for nerve contact, and were additionally coated with iridium oxide materials to enhance the stimulation performance of the device. After the implantation, the two coated electrodes were in parallel contact over the nerve surface. The detailed fabrication and coating processes are described in the supplementary section S2 and S3.

Different stimulation parameters such as pulse width, amplitude, and frequency generated by the proposed device are applied for pelvic nerve stimulation to demonstrate bladder modulation. For pelvic nerve stimulation, biphasic square pulses of short pulse width (a few hundred seconds) with multiple train pulses are typically applied [46,47]. Therefore, the effect of relatively long pulse width and exponential waveforms on bladder stimulation should be preferentially demonstrated. For this, we demonstrate comparative studies of pelvic nerve stimulation using commercial stimulation depending on low amplitudes and long pulse width.

3. Characterization of triboelectric stimulator

The prepared 4-layer TENGs were characterized with a constant force (40 N). The layers were connected in parallel to maximize output current [20]. We measured the short circuit current of the device since the impedance of the implanted neural interface on a pelvic nerve was around a few tens of kilo-ohms. This is negligible compared with the internal impedance of the TENG that was around tens of mega-ohms [20]. Different frequencies of hand-tapping were manually performed within the range for 25 to 150 BPM (Beat per minute) that is compatible with one hand. Firstly, the device with the size of 4 × 4 cm (contact area: 16 cm^2) was demonstrated to generate electrical energy. The output currents were recorded depending on BPM of 25, 50, 100, and 150 (Fig. 2a–d). Actual BPMs were calculated with the intervals of the recorded peak signals, which were 25.2 (n = 5), 50. 1 (n = 5), 103.9 (n = 5), and 153.5 (n = 5) BPMs, respectively.

To characterize the detailed stimulation parameters such as pulse width, current, and shape of pulses, each pulse generated by TENGs was analyzed. Each pulse had a major biphasic waveform following a minor biphasic waveform (Fig. 2e). The result of the output current generated by a hand at 50 BPM. The positive peak current of the major waveform was 5.4 ± 0.64 μA (n = 5) and the negative peak current of the major waveform was 2 ± 0.48 μA (n = 5). The positive and negative peak currents of the minor waveform were 0.66 ± 0.39 μA (n = 5) and 0.51 ± 0.27 μA (n = 5), respectively. The minor peak currents (< 1 μA) were very small, and are less than motor nerve's rheobase current that is defined as the threshold current for infinitely long pulses, so that these minor waveforms could be negligible [45,48]. The shape of the major positive pulse was relatively sharp, and narrower than the one for the major negative pulse. The major positive pulse seemed to be the leading phase for stimulation waveforms, and the major negative pulse seemed to be the returning phase for a charge-balanced waveform. The pulse widths of the pulses were also characterized. The pulse widths of major positive and negative pulses were 15.7 ± 1.01 ms (n = 5) and 43.2 ± 2.39 ms (n = 5), respectively. The pulse widths of minor positive and negative pulses were 2.37 ± 1.39 ms (n = 5) and 4.77 ± 3.52 ms (n = 5), respectively.

The pulse width of 15 ms seemed to be larger than the typical pulse width for stimulation in the case where a rectangle pulse was applied. However, the wave shape of the device was close to an exponential waveform. Accordingly, we calculated charge per pulse based on the peak current and the pulse width to verify actual charge delivered. Due to the unique characteristics of TENG, the charge sum of a positive pulse and a negative pulse is zero. Therefore, it can be expressed by Ref. [22],

$$\int I_p(t_p)dt_p = \int I_n(t_n)dt_n$$

where I_p is the current of the major positive pulse, t_p is the time of the major positive pulse, I_n is the current of the major negative pulse, and t_n is the time of the major negative pulse.

The calculated total charge output was 29.5 nC (n = 5) per pulse. This value was reasonable for electrical stimulation based on previous studies [23,24]. In addition, the charge of the minor waveform was less than 1 nC, so we concluded that the minor waveform could not influence the stimulation.

This kind of charge-balanced current waveform has the advantage of avoiding damage to electrodes and surrounding tissue [22,24]. For instance, deep brain stimulation (DBS) devices deliver asymmertrical biphasic stimulation pulses with a leading cathodic phase followed by a longer, charge-balancing, anodic phase. And the low-amplitude anodic phase lags the cathodic phase so that it cannot exert a conditioning effect [48]. Here, the data was presented anodic phase first and followed a cathodic phase. However, the FNS had two sensing electrodes that were positioned in parallel to the direction of the pelvic nerve after implantation so that the phase can be controlled inversely. Therefore, we assume that the major positive pulse was the leading phase of the stimulation, and the major negative pulse was the returning phase.

Major pulse widths and major peak currents depending on the BPM were investigated in Fig. 2 f and g. The positive pulse widths showed smaller variation from 14.67 ms to 15.7 ms depending on BPM while the negative pulse width presented wider variation from 37.5 ms to 44 ms (Fig. 2f). This is possibly because a constant pushing speed contributing to the generation of the positive pulse widths is well controlled by a hand, while releasing speed of the device associated with negative pulse widths is related to the resilience property of PET materials. Large BPM may not provide enough time to release the layers completely. Positive peak current generated by 25 BPM was 4.59 ± 0.81 μA (n = 5), and it was increased with the increase in BPM until 100 BPM (6.27 ± 0.43 μA (n = 5)). At 150 BPM, positive current was 5.91 ± 0.69 μA (n = 5), which was slightly less than one generated by 100 BPM, and it seems to be saturated. This may also be due to layers that are not completely separated. At 100 BPM, positive current showed the highest value, which may be due to the large force applied naturally when applying large BPM. Negative peak current generated by 25 BPM was 1.65 ± 0.459 μA (n = 5), and it was increased with the increase in BPM 150 BPM which was 2.1 ± 0.13 μA (n = 5). Again, discussed above, negative pulses are returning phase in a charge-balance waveform, so we assume that it does not seriously affect for the stimulation.

4. Bladder modulation dependence on stimulation frequency

Electrical stimulation of bladder pelvic nerve using the TENGs was performed. To investigate the effect of stimulation frequency on bladder modulation, we delivered different BPM of stimulation signals for 5 s. Firstly, we implanted the prepared clip interface on a pelvic

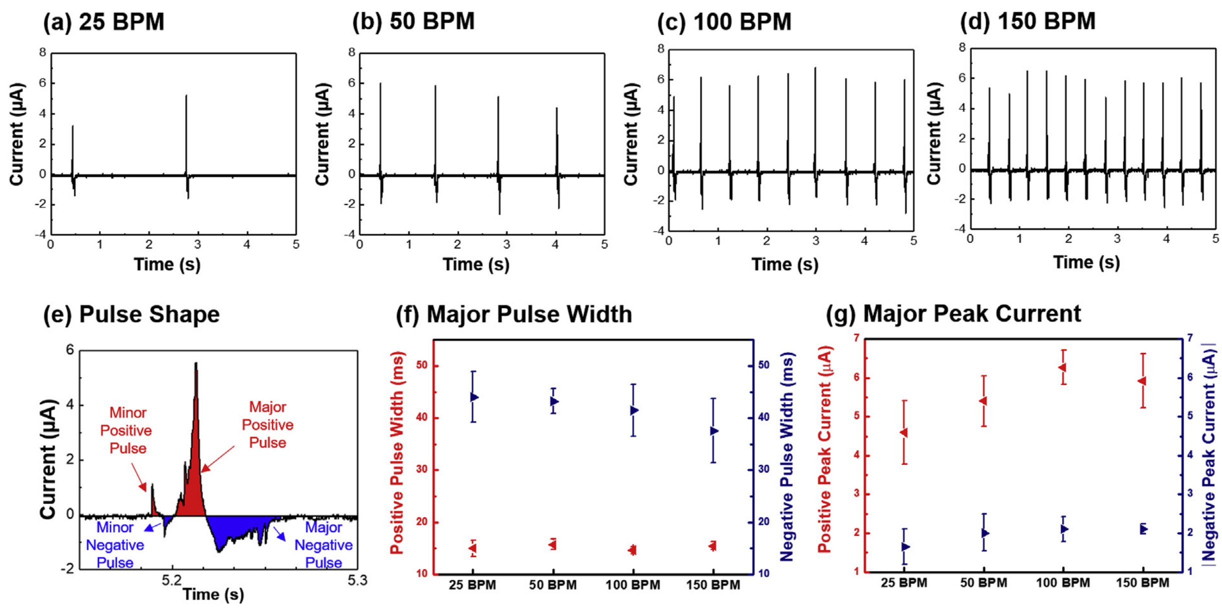

Fig. 2. Characterization of TENG. Output currents generated by the TENG depending on beat per minutes (BPM), (a) 25, (b) 50, (c) 100, and (d) 150 BPM. (e) The component and shape of biphasic pulses generated by TENGs. (f) Pulse width of the major pulse depending on BPM. (g) Peak currents of the major pulse depending on BPM.

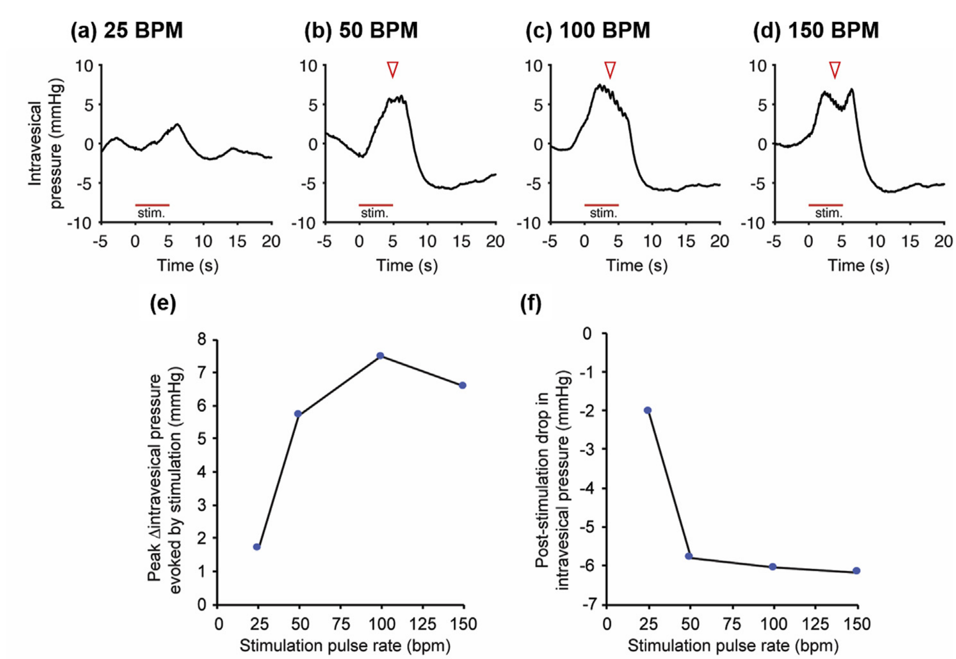

Fig. 3. Mechano-bladder stimulation and bladder pressure change depending on stimulation frequency. Intravesical bladder pressure changes depending on mechano-bladder stimulation with (a) 25, (b) 50, (c) 100, and (d) 150 Beat per minutes (BPM). Inverted triangles denote the voiding events. (e) Pressure changes while the stimulation depending on BPM. (f) Post-stimulation drop in intravesical pressure while the stimulation depending on BPM.

nerve of a rat that is located right beside the bladder. After the identification of the nerve, then we stimulated the pelvic nerve using a commercial stimulator to check the functionality of the interface, as well as the measurement setup for the bladder contraction. After that, the TENG was connected to the clip interface. We applied the different BPM of 25, 50, 100, and 150 for the stimulation of the nerve while monitoring intra-bladder pressure and micturition. When applying to 25 BPM to the nerve for the stimulation, small change in bladder pressure was observed, but there was no micturition (Fig. 3a). At the stimulation of 50 BPM, clear bladder changes in the pressure were observed with micturition (Fig. 3b). In addition, stimulation with 100 and 150 BPM induced the occurrence of micturition and larger pressure changes than previous ones (Fig. 3c and d). Peak pressure changes also showed that the stimulation by 25 BPM caused small change (< 2 mmHg) while the stimulation by 50, 100, and 150 BPM led to larger change (> 5 mmHg) (Fig. 3e). Post-stimulation drop in intravesical pressure, which is relevant to the occurrence of micturition, showed significantly larger pressure drops above 50 BPM [47]. This trend is consistent with the tendency of the major positive peak current change depending on BPM (Fig. 2g). The low current around 4 μA at 25 BPM and a small number of pulses (2 pulses) might be the phenomena of small bladder pressure change without micturition. This also indicates that the rheobase current when to apply the current by the suggested device is around 4 μA. This also support the assumption that the low currents (1–2 μA) of negative pulses are returning phase in a charge-balance waveform, which cannot seriously affect for the stimulation.

These results demonstrate that this mechano-neuromodulation combined with the FNC and the TENG can induce bladder contraction for micturition. A video demonstration of bladder modulation can be

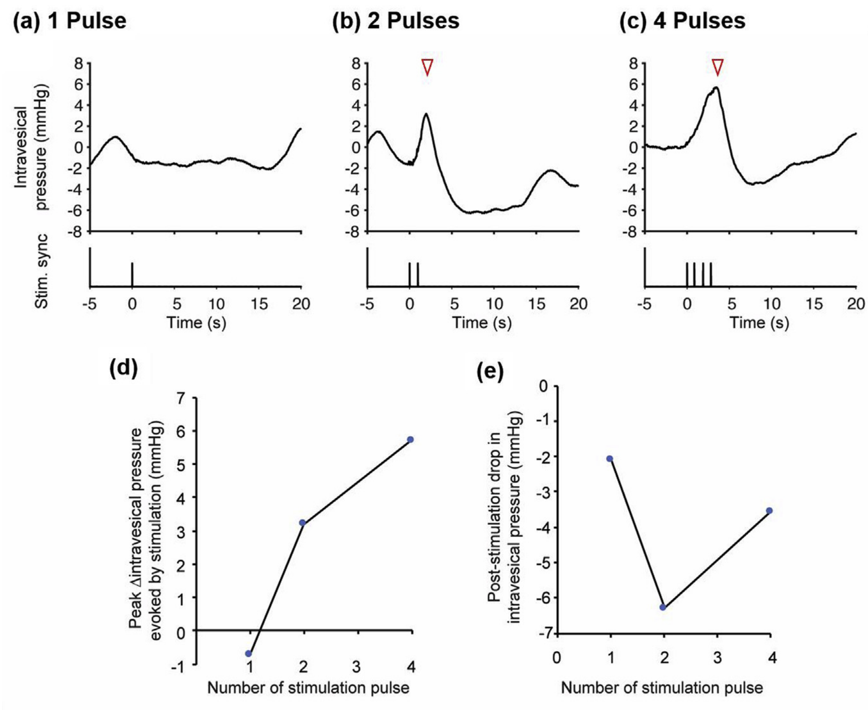

Fig. 4. Mechano-bladder stimulation and bladder pressure change depending on number of stimulation pulse. Intravesical bladder pressure changes depending on mechano-bladder stimulation with (a) 1, (b) 2, and (c) 4 pulses. Inverted triangles denote the voiding events. (d) Pressure changes while the stimulation depending on number of pulse. (e) Post-stimulation drop in intravesical pressure while the stimulation depending on number of pulse.

found in Supplementary information.

Supplementary video related to this article can be found at https://doi.org/10.1016/j.nanoen.2019.03.082.

5. Bladder modulation dependent on number of stimulation pulses

To investigate the dependence on number of stimulation pulse, we applied different number of pulses (1–4 pulses) to pelvic nerves in rats. We manually applied the same force (40 N) at 50 BPM to the TENG that was used for the characterization of the TENG. This is because that the stimulation by 50 BPM showed good results of the pressure change and the micturition in previous experiment, as well as 50 BPM is precisely manageable by a hand (50.1 BPM). Fig. 4a shows changes in bladder pressure when one pulse was applied. There was no change in bladder pressure or any other physiological response. However, we observed large bladder pressure changes when more than two pulses were applied. The clear change in the baseline pressure before and after stimulation was observed when applying to two pulses in Fig. 4b. When we applied to three pulses, there was no clear baseline change, but we observed a small amount of micturition. When applying to four pulses, the clear shape of bladder pressure change was observed as shown in Fig. 4c, indicating that a voiding event occurred [25]. Fig. 4d shows peak bladder pressure changes depending on number of stimulation pulses. Two and four pulses stimulation also caused larger pressure drops, corroborating the visual observation of urine output from the meatus, when compared to single pulse stimulation. In Fig. 4e, although both 2 and 4 stimulation pulses evoked voiding responses, the smaller post-stimulation drop evoked by 4 stimulation pulses suggests that a corresponding strong external urethral sphincter contraction was also evoked, thus decreasing the voiding efficiency. A previous study had shown that stimulation of pelvic nerve, which is a mixed nerve containing both parasympathetic efferents and sensory afferents, can evoked both bladder contraction and external sphincter contraction [47]. The result indicates that one pulse (29.5 nC) delivered less than the required energy for the activation while more than two pulses (> 59 nC) conveyed suprathreshold energy for the stimulation using this technology.

6. Comparison of bladder stimulation by commercial stimulator

Bladder stimulation applied long pulse width (tens of milliseconds) using a commercial stimulator was performed to investigate physiological response of bladder modulation. Firstly, we applied normal stimulation parameters that were used for the study of bladder stimulation in previous studies [45–47]. Intravesical pressure change while the stimulation was shown in Fig. 5a. Stimulation parameters with biphasic square waveforms were amplitude of 100 μA, pulse width of 150 μs, and interpulse period of 100 ms for 5 s (Fig. 5b). The clear pressure change and micturition were observed. Considering only one phase pulse (negative pulse) affects the stimulation, total charge delivered to the pelvic nerve was 750 nC for 5 s. After that, long pulse width of 80 ms was applied for bladder stimulation. The interpulse period of 250 ms and 5 s stimulation were fixed, and amplitude was increased from 1 to 5 μA. When applying 1 μA while the stimulation, there was small pressure change, but no clear micturition occurred (Fig. 5c). Ideally, total charge delivered to the stimulation was 1600 nC, but there was no clear response. At the amplitude of 3 μA, noticeable pressure change and small amount of urine was observed (Fig. 5d). However, the shape of pressure change was unusual compared with ones under the other stimulation conditions. Clear pressure change and clear micturition were observed with stimulation amplitude of 5 μA (Fig. 5e). This demonstrates that low amplitudes and long pulse widths by a commercial stimulator could also drive micturition despite lower positive pressure changes.

7. Chronic implantation of neural clip interface

One of challenges in long-term use of neuro-stimulator is chronic implantation of electrodes (or lead). Most of all, conformal implantation and close contact of electrode are critical to deliver designed stimulation parameters. Furthermore, chronic implantation of electrodes usually causes the performance degradation or functionality failure due to the generation of scar tissue as a foreign body reaction.

Chronic implantation of the clip interface was performed to validate long-term implantation of the clip interface. Neural clip interfaces were implanted on bladder pelvic nerves in rats for 16 days. Firstly, the clip interface was implanted on the pelvic nerve, then the nerve was

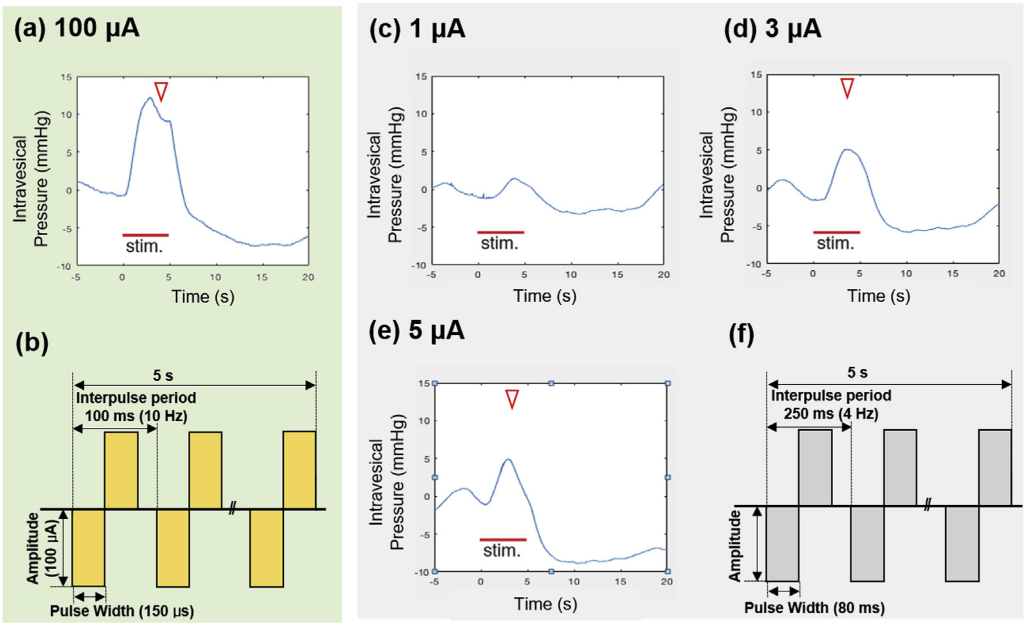

Fig. 5. Comparison of bladder stimulation by commercial stimulator. (a) Intravesical pressure change while the stimulation with amplitude of 100 μA. (b) Schematic diagram of biphasic stimulation pulses with pulse width of 150 μs and interpulse period of 100 ms for 5 s. Intravesical pressure changes while the stimulation with amplitude of (c) 1, (d) 3, and (e) 5 μA. (f) Schematic diagram of the biphasic stimulation pulses with pulse width of 80 ms and interpulse period of 250 ms for 5 s. Inverted triangles denote the voiding events.

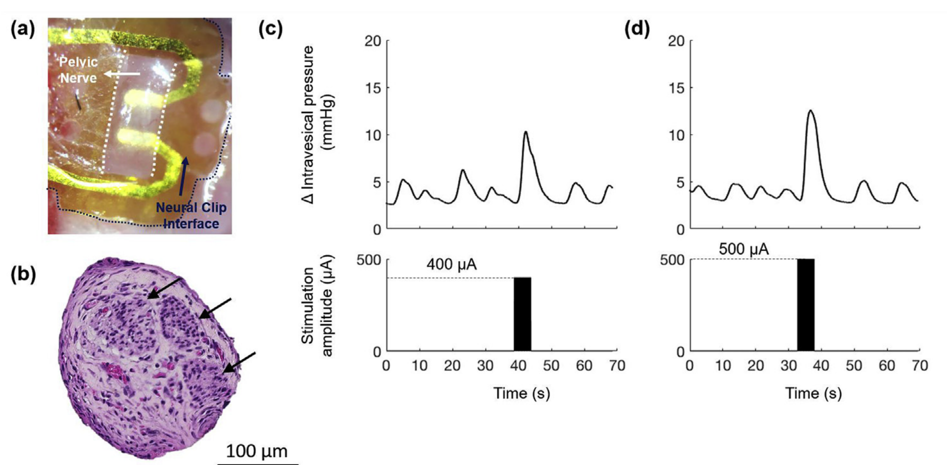

Fig. 6. Chronic implantation of flexible neural clip (FNC) on pelvic nerves of rat. (a) Photomicrograph of FNC on pelvic nerves 16 days after chronic implantation. Photomicrograph of pelvic nerves shown in (b) sectioned in the transverse plane and stained with hematoxylin and eosin (H&E). Black arrows indicate pelvic nerve branches. Intravesical bladder pressure changes in response to electrical stimulation of 400 μA (c) and 500 μA (d) delivered to pelvic nerves through the FNC 16-days post implantation.

stimulated via the interface to check electrode and nerve functionality (100–500 μA). The bladder contraction was observed, then the surgical site was sutured. After 16 days, to verify the health of the pelvic nerve, we opened the surgical site and check the condition of the pelvic nerve in anesthetized rat. The clip electrode was observed to be physically interfacing with the nerve, although the macroscopic appearance of the nerve suggested some degree of foreign body reaction (Fig. 6a). Histological analysis showed that individual pelvic nerve branches were still identifiable at the nerve-electrode interface, although some scar tissues had also formed around the nerve branches. When we performed electrical stimulation of the pelvic nerve through the same electrode implant at 400 μA while monitoring intravesical bladder pressure, positive bladder pressure change was observed (Fig. 6c). The positive intravesical change further increased when larger stimulation current of 500 μA was used (Fig. 6d). These results indicate that the chronically-interfaced pelvic nerve preserved sufficient functionality to evoked bladder contractions when stimulated.

8. Concluding remarks

We demonstrated mechano-neuromodulation of autonomic pelvic nerve for bladder function in rats using a triboelectric neurostimulator integrated with a flexible neural clip interface. The characteristics of the TENG were investigated in terms of current, pulse width, and charge for the *in vivo* experiments. The unique mechanism of TENGs provided current with a charge-balanced waveform that had the benefit of reducing damage to electrodes and tissues. The overall pulse widths were larger than the typical ones for stimulation, but the exponential shape of the pulse delivered a reasonable charge for stimulation (~29.5 nC per pulse).

During *in vivo* experiments, we demonstrated the dependence of frequency (based on BPM) and number of pulses on bladder modulation. Different BPM (25, 50, 100, 150 BPM) pulses were delivered to the pelvic nerve for the stimulation while monitoring physiological responses such as intravesical pressure in bladder and micturition. Stimulation by more than 50 BPM showed clear bladder contraction and micturition events. In the experiment of number of pulses dependent stimulation, bladder contractions with micturition were observed, except for one case when only one pulse was applied. Most of the changes in bladder pressure showed clear changes in the baseline pressure, indicating typical physiological responses. The results demonstrate that too low frequency (< 0.4 Hz; 25 BPM) stimulation may be not enough to evoke bladder contraction. In addition, surprisingly, applying only two pulses with around 1 Hz (0.83 HZ; 50 BPM) is sufficient to generate micturition response using this technology. For the comparison of bladder stimulation by a commercial stimulator, long pulse width (80 ms) with very low amplitude of 1, 3, and 5 μA were applied for the bladder stimulation, respectively. The stimulation by more than 3 μA showed bladder pressure changes and micturition indicating that long pulse stimulation does work for bladder modulation. This result also indicates that the rheobase current is less than 3 μA for a pelvic nerve when applying biphasic pulses by a commercial stimulator. Again, this result supports our assumption of the negligible minor peak currents that were less than 1 μA. Finally, chronic implantation of flexible clip interface was demonstrated. After 16-days implantation, the FNC maintained the stimulation functionality of bladder modulation without damage in the pelvic nerve.

All results demonstrate that this mechano-neuromodulation technology can induce bladder contraction with micturition showing promising possibility of mechano-neuromodulation. Furthermore, it opens the possibility of modulating other autonomic nerves using this technology for bioelectronic medicine.

The next step will be demonstration of the long-term physiological effect on bladder and pelvic nerve when applying this stimulation technology. Furthermore, advanced versions of TENG need to be developed. For instance, a biocompatible package of device will be required for implantable devices to maintain the performance of the device in harsh *in vivo* environments. Furthermore, bionic design of the device associated the movement of muscles and organs will be great for stable and self-sustainable performance. It would be great to extend the range of uses of various mechanical energy derived from the skin or the internal body.

Acknowledgements

This work was supported by grants from the National Research Foundation (NRF) CRP project 'Peripheral Nerve Prostheses: A Paradigm Shift in Restoring Dexterous Limb Function' (R-719-000-001-281), and HIFES Seed Funding-2017-01 grant (R-263-501-012-133) "*Hybrid Integration of Flexible Power Source and Pressure Sensors*" at the National University of Singapore; The DGIST Start-up Fund Program of the Ministry of Science and ICT (2019010072), the National Research Foundation of Korea (2019R1C1C1008344).

Appendix A. Supplementary data

Supplementary data to this article can be found online at https://doi.org/10.1016/j.nanoen.2019.03.082.

References

[1] S. Huang, Y. Liu, Y. Zhao, Z. Ren, C.F. Guo, Adv. Funct. Mater. (2018) 29.
[2] S. Lee, Q. Shi, C. Lee, Apl. Mater. 7 (2019).
[3] Q. Shi, T. He, C. Lee, *Nano* Energy 57 (2019) 851–871.
[4] W. Khan, M. Setien, E. Purcell, W. Li, Front. Mech. Eng. 4 (2018).
[5] B. Ji, M. Wang, X. Kang, X. Gu, C. Li, B. Yang, X. Wang, J. Liu, IEEE Trans. Electron Devices 64 (2017) 2008–2015.
[6] J. Xu, S. Wang, G.J.N. Wang, C. Zhu, S. Luo, L. Jin, X. Gu, S. Chen, V.R. Feig, J.W.F. To, S. Rongdeau-Gagne, J. Park, B.C. Schroeder, C. Lu, J.Y. Oh, Y. Wang, Y.H. Kim, H. Yan, R. Sinclair, D. Zhou, G. Xue, B. Murmann, C. Linder, W. CAi, J.B.H. Tok, J.W. Chung, Z. Bao, Science 355 (2017) 59–64.
[7] X. Wang, Y. Gu, Z. Xiong, Z. Cui, T. Zhang, Adv. Mater. 26 (2014) 1336–1342.
[8] Y. Li, Y. Ma, C. Wei, H. Luan, S. Xu, M. Han, H. Zhao, C. Liang, Q. Yang, Y. Yang, K.E. Crawford, X. Feng, Y. Huang, J.A. Rogers, Adv. Funct. Mater. (2018) 28.
[9] W. Gao, S. Emaminejad, H.Y.Y. Nyein, S. Challa, K. Chen, A. Peck, H.M. Fahad, H. Ota, H. Shiraki, D. Kiriya, D.H. Lien, G.A. Brooks, R.W. Davis, A. Javey, Nature 529 (2016) 509–514.
[10] H. Wang, G. Pastorin, C. Lee, Adv. Sci. 3 (2016) 1500441.
[11] H. Wang, Z. Xiang, P. Giorgia, X. Mu, Y. Yang, Z.L. Wang, C. Lee, *Nano* Energy 23 (2016) 80–88.
[12] D. Pani, A. Dessi, J.F. Saenz-Cogollo, G. Barabino, B. Fraboni, A. Bonfiglio, IEEE Trans. Biomed. Eng. 63 (2016) 540–549.
[13] L. Chen, Q. Shi, Y. Sun, T. Nguyen, C. Lee, S. Soh, Adv. Mater. 30 (2018) e1802405.
[14] J.H. We, S.J. Kim, B.J. Cho, Energy 73 (2014) 506–512.
[15] H. Liu, J. Zhong, C. Lee, S.-W. Lee, L. Lin, Appl. Phys. Rev. 5 (2018).
[16] Z. Xiang, S. Sheshadri, S.H. Lee, J. Wang, N. Xue, N.V. Thakor, S.C. Yen, C. Lee, Advanced Science 3 (2016) 1500386.
[17] J. Wang, X.Y. Thow, H. Wang, S. Lee, K. Voges, N.V. Thakor, S.C. Yen, C. Lee, Adv. Healthc. Mater. 7 (2017) 1700987.
[18] Z. Xiang, S.C. Yen, S. Sheshadri, J. Wang, S. Lee, Y.H. Liu, L.D. Liao, N.V. Thakor, C. Lee, Adv. Mater. 28 (2016) 4472–4479.
[19] S. Lee, C. Lee, Current Opinion in Biomedical Engineering 6 (2018) 130–137.
[20] M.-H. Wang, B.-W. Ji, X.-W. Gu, Z.-J. Guo, X.-L. Wang, B. Yang, C.-Y. Li, J.-Q. Liu, Sensor. Actuator. B Chem. 264 (2018) 100–109.
[21] X.S. Zhang, M.D. Han, R.X. Wang, B. Meng, F.Y. Zhu, X.M. Sun, W. Hu, W. Wang, Z.H. Li, H.X. Zhang, *Nano* Energy 4 (2014) 123–131.
[22] J. Wang, H. Wang, N.V. Thakor, C. Lee, ACS Nano 13 (2019) 3589–3599.
[23] Y. Long, H. Wei, J. Li, G. Yao, B. Yu, D. Ni, A.L. Gibson, X. Lan, Y. Jiang, W. Cai, X. Wang, ACS Nano 12 (2018) 12533–12540.
[24] W. Hu, X. Wei, L. Zhu, D. Yin, A. Wei, X. Bi, T. Liu, G. Zhou, Y. Qiang, X. Sun, Z. Wen, Y. Pan, Nano Energy 57 (2019) 600–607.
[25] G. Yao, L. Kang, J. Li, Y. Long, H. Wei, C.A. Ferreira, J.J. Jeffery, Y. Lin, W. Cai, X. Wang, Nat. Commun. 9 (2018) 5349.
[26] Z. Liu, J. Nie, B. Miao, J. Li, Y. Cui, S. Wang, X. Zhang, G. Zhao, Y. Deng, Y. Wu, Z. Li, L. Li, Z.L. Wang, Adv. Mater. (2019) e1807795.
[27] S. Lee, H. Wang, J. Wang, Q. Shi, S.-C. Yen, N.V. Thakor, C. Lee, Nano Energy 50 (2018) 148–158.
[28] W. Yang, W. Khan, J. Wu, W. Li, J. Micromech. Microeng. 29 (2019).
[29] S. Lee, H. Wang, Q. Shi, L. Dhakar, J. Wang, N.V. Thakor, S.-C. Yen, C. Lee, Nano Energy 33 (2017) 1–11.
[30] F. Arab Hassani, R.P. Mogan, G.G.L. Gammad, H. Wang, S.C. Yen, N.V. Thakor, C. Lee, ACS Nano 12 (2018) 3487–3501.
[31] Q. Zheng, B. Shi, Z. Li, Z.L. Wang, Adv. Sci. 4 (2017) 1700029.
[32] N. Li, Z. Yi, Y. Ma, F. Xie, Y. Huang, Y. Tian, X. Dong, Y. Liu, X. Shao, Y. Li, L. Jin, J. Liu, Z. Xu, B. Yang, H. Zhang, ACS Nano 13 (2019) 2822–2830.
[33] W. Jiang, H. Li, Z. Liu, Z. Li, J. Tian, B. Shi, Y. Zou, H. Ouyang, C. Zhao, L. Zhao, R. Sun, H. Zheng, Y. Fan, Z.L. Wang, Z. Li, Adv. Mater. 30 (2018) e1801895.
[34] H. Feng, C. Zhao, P. Tan, R. Liu, X. Chen, Z. Li, Adv. Healthc. Mater. 0 (2018) 1701298.
[35] B. Shi, Z. Li, Y. Fan, Adv. Mater. 30 (2018) e1801511.
[36] Q. Zheng, Y. Zou, Y. Zhang, Z. Liu, B. Shi, X. Wang, Y. Jin, H. Ouyang, Z. Li, Z.L. Wang, Sci Adv 2 (2016) e1501478.
[37] A. Gammie, M. Kaper, C. Dorrepaal, T. Kos, P. Abrams, Eur. Urol. 69 (2016) 361–369.
[38] F.A. Hassani, G.G.L. Gammad, R.P. Mogan, T.K. Ng, T.L.C. Kuo, L.G. Ng, P. Luu, N.V. Thakor, S.-C. Yen, C. Lee, *Adv. Mater. Technol.* 3 (2018).
[39] F.A. Hassani, W.Y.X. Peh, G.G.L. Gammad, R.P. Mogan, T.K. Ng, T.L.C. Kuo, L.G. Ng, P. Luu, S.C. Yen, C. Lee, Adv. Sci. 4 (2017) 1700143.
[40] P.T. Dorsher, P.M. McIntosh, Adv Urol 2012 (2012) 816274.
[41] K. Famm, B. Litt, K.J. Tracey, E.S. Boyden, M. Slaoui, Nature 496 (2013) 159–161.
[42] I. Adameyko, Science 354 (2016) 833–834.
[43] W.C. Groat, C. Tai, Bioelectron Med 22 (2015) 25–36.
[44] N.B.N. Trust, (2016).
[45] S. Lee, W.Y.X. Peh, J. Wang, F. Yang, J.S. Ho, N.V. Thakor, S.C. Yen, C. Lee, Adv. Sci. 4 (2017) 1700149.
[46] W.Y.X. Peh, M.N. Raczkowska, Y. Teh, M. Alam, N. Thakor, S.C. Yen, J. Neural Eng. 15 (2018) 066009.
[47] W.Y.X. Peh, R. Mogan, X.Y. Thow, S.M. Chua, A. Rusly, N.V. Thakor, S.C. Yen, Front. Neurosci. 12 (2018) 186.
[48] D.T. Brocker, W.M. Grill, Handb. Clin. Neurol. 116 (2013) 3–18.

Sanghoon Lee is an Assistant Professor in the Department of Robotics Engineering, Daegu Geongbuk Institute of Science and Technology (DGIST). And he is the director of Neuro-Interfaced Robotics Lab. He received the B.S. degree at the Department of Electronic Material Engineering, Kwangwoon University, Seoul, Korea in 2009 and his M.S. and Ph.D. degrees at the Department of Electrical and Computer Engineering (ECE), National University of Singapore (NUS) in 2013 and in 2017, respectively. His research interests are in advanced neural interface and relevant to robotic systems for neuroprosthetics and bioelectronic medicines.

Hao Wang received his B.Eng. degree in School of Optoelectronic Information from University of Electronic Science and Technology of China in 2010 and received his Ph.D. degree from the Department of Electrical and Computer Engineering, National University of Singapore (NUS) in 2016. He is currently a Research Fellow of ECE, NUS. His research interests are focused on nanoneedle devices for transdermal drug delivery, flexible and wearable electronics, energy harvesting and electrical neural stimulations.

Wendy Peh is a Research Fellow at the Singapore Institute for Neurotechnology (SINAPSE), National University of Singapore (NUS). She received her Ph.D. degree from Duke University, Department of Neurobiology, U.S. in 2014. Her research focuses on neuromodulation of peripheral nerves innervating visceral organs such as bladder for recovery of physiological function.

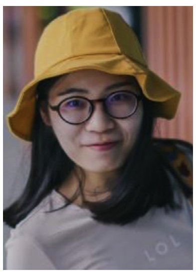

Tianyiyi He received her B.Eng. degree from the School of Microelectronics and Solid-state Electronics at the University of Electronic Science and Technology of China (UESTC), Chengdu, China, in 2016. She is now a Ph.D. candidate in the Department of Electrical and Computer Engineering, National University of Singapore. Her research interests focus mainly on thermoelectrics.

Shih-Cheng Yen received his B.S.E. and M.S.E. in 1993, and his Ph. D. in 1998, all from the Department of Bioengineering at the University of Pennsylvania. For his Ph.D, he worked on neural network models of the primary visual cortex. He was a Research Assistant Professor at Montana State University. He is currently an Assistant Professor in the Department of Electrical and Computer Engineering at the National University of Singapore (NUS), and was the Deputy Director of the Singapore Institute for Neurotechnology (SINAPSE) at NUS. His research interests are in neural coding and neuroprosthetics.

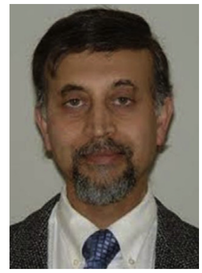

Nitish V. Thakor is the Professor of Electrical and Computer Engineering and Biomedical Engineering. Previously, he was the Director the Singapore Institute for Neurotechnology (SINAPSE) at the National University of Singapore, and was the Professor of Biomedical Engineering at Johns Hopkins University. Prof. Thakor's technical expertise is in the field of Neuroengineering, where he has pioneered many technologies for brain monitoring to prosthetic arms and neuroprosthesis. He is currently the Editor in Chief of Medical and Biological Engineering and Computing, and was the Editor in Chief of IEEE TNSRE from 2005 to 2011.

Chengkuo Lee received his Ph.D. degree in Precision engineering from The University of Tokyo in 1996. Currently, he is the director of Center for Intelligent Sensors and MEMS, and an Associate Professor in the Department of Electrical and Computer Engineering, National University of Singapore, Singapore. In 2001, he cofounded Asia Pacific Microsystems, Inc., where he was the Vice President. From 2006 to 2009, he was a Senior Member of the Technical Staff at the Institute of Microelectronics, A-STAR, Singapore. He has contributed to more than 300 international conference papers and extended abstracts and 290 peer-reviewed international journal articles.